



Published in final edited form as:

Precis Radiat Oncol. 2018 December ; 2(4): 106–113. doi:10.1002/pro6.55.

Monte Carlo calculation of the mass stopping power of EBT3 and EBT-XD films for protons for energy ranges of 50–400 MeV

Chengyu Shi¹, Chin-Cheng Chen², Dennis Mah², and Maria F. Chan¹

¹Department of Medical Physics, Memorial Sloan Kettering Cancer Center, Basking Ridge, New Jersey, USA

²Department of Radiation Physics, ProCure Proton Center, Somerset, New Jersey, USA

Abstract

Objective: The goal of the present study was to calculate the continuous slowing down approximation (CDSA) ranges and derive mass stopping power for EBT3 and EBT-XD films for therapeutic protons energy ranges of 50–400 MeV.

Methods: The MCNPX and TRansport of Ions in Matter (TRIM) Monte Carlo codes were used in this study. Utilizing the published International Commission on Radiation Units and Measurement 49 data for the water mass stopping power and CSDA ranges, the mass stopping powers of EBT3 and EBT-XD films were derived using the approximation proposed by Newhauser and Zhang in 2009.

Results: The calculated CSDA ranges by MCNPX and TRIM in water were first benchmarked to International Commission on Radiation Units and Measurement 49 published data for water, and found to be within 1% with a 1.4-mm maximum difference. The calculated CSDA values in EBT3 film, compared with the measured CSDA ranges in the EBT3 film, were within 2% of the calculated values with a 3-mm maximum difference. The MCNPX and TRIM results for CSDA ranges agreed with each other to within 2.7% for EBT3 film and 4.4% for EBT-XD film. The overall uncertainties of the MCNPX and TRIM-derived CSDA ranges were 3% and 1.3%, respectively.

Conclusion: The mass stopping powers for Gafchromic EBT3 and EBT-XD films were derived.

Keywords

EBT-XD; EBT3; film dosimetry; mass stopping power; proton

This is an open access article under the terms of the Creative Commons Attribution-NonCommercial-NoDerivs License, which permits use and distribution in any medium, provided the original work is properly cited, the use is non-commercial and no modifications or adaptations are made.

Correspondence Chengyu Shi, Memorial Sloan Kettering Cancer Center, 480 Red Hill Road, Middletown, NJ 07748, USA. shic@mskcc.org.

CONFLICT OF INTEREST

The authors declare that they had read the article and there are no competing interests.

1 INTRODUCTION

Film dosimetry is an important method for the measurement of radiation. There has been extensive research carried out on EBT and EBT2 films. For instance, Monte Carlo calculation of mass energy absorption coefficients and restricted stopping power ratios of water to active film materials of EBT and EBT2 films for photons has been reported by Sutherland and Rogers.¹ Zhao and Das found that EBT film is suitable for measuring the proton beam range; however, the film response is a function of energy over the effective (film vs ion chamber measurements for percentage depth doses [PDD]) proton energy of 50–160 MeV with under-response of PDD in film <10% compared with an ion chamber.² Under-response of up to 20% was observed at the peak of the Bragg curve. Kirby *et al.* carried out work to use stopping power to calculate a factor and account for the beam quality changing with depth in proton beams measured using EBT film.³

The new film types, EBT3 and EBT-XD, have been introduced to the market in recent years. The most prominent improvements of EBT3 films are the symmetric structure to reduce face-up/down dependency, as well as the special surface coating to prevent Newton's ring artifacts.⁴ Later EBT-XD, similar in composition and construction to EBT3, was produced with a reduced crystal size of the active component of this film, which makes it less sensitive. However, the increased slope of the dose–response curve at doses >10 Gy make it more suitable for high-dose measurements.^{5–10} Perles *et al.* followed Kirby's work³ and calculated linear energy transfer correction factors using stopping powers for EBT2/EBT3 films.¹¹ Goma *et al.* found that water/medium stopping power ratios for protons in radiochromic film as a function of depth in water are quite constant (within 2.5%).¹² They also used distal R_{80} (80% of maximum Bragg peak) as the proton beam range. Fiorini *et al.* also used a water-to-film stopping power ratio concept to correct the dose measurement of a 29-MeV modulated proton beam.¹³ Jung *et al.* applied a single stopping power ratio for correcting EBT3 measurements in heterogeneous regions.¹⁴ Battaglia *et al.* measured EBT3 film response to a 3-MV proton beam and used mass stopping power to correct the dose measured in the film.¹⁵ However, there have been very few studies involving proton beams using stopping powers; in particular, a full range of stopping power values in EBT3 and EBT-XD is not available in the literature.

Proton therapy has the advantage of sparing healthy tissues by utilizing the Bragg peak and the finite range of the beam; radiation almost completely stops before hitting the healthy tissues, thereby delivering a lower dose to the healthy tissues.¹⁶ Gafchromic films have also proven to be an effective way to determine proton beam PDD, lateral dose profiles, and plan verification.² In order to convert the absorbed dose in film to that in water, it is necessary to know the mass stopping power values for the films. Although the International Commission on Radiation Units and Measurement (ICRU) Report 49¹⁷ and the latest ICRU 90¹⁸ publish the mass stopping power and ranges of protons, with earlier Gafchromic film models, values for newer models, such as EBT3 and EBT-XD, are not available. Therefore, it is essential to determine those mass stopping power values for clinical applications. The mass stopping powers are essential data that can be calculated using theory or measured by experiments;¹⁷ however, it might be time-consuming or lack the required accuracy. In contrast, Monte Carlo simulation of the proton range is now more mature as a technique.

Based on the range's results, one can derive the proton mass stopping power values based on the water equivalent ratio equation of water to the film.¹⁹ Although the equation of Zhang and Newhauser is based on a thin target assumption,¹⁹ it can be extended into clinical applications with sufficient accuracy, because there is only a weak dependence on the target thickness.¹⁶ Therefore, the continuous slow-ing down approximation (CSDA) range (g/cm^2), simulated or measured, can be used to derive the water equivalent ratio and further drive the mass stopping power of the film.

In the present study, the CSDA ranges of different monoenergetic proton energies in EBT3 and EBT-XD films were calculated for the energy range of 50–400 MeV. The mass stopping power ratios of the media (film) to water were derived based on the ICRU report 49 water mass stopping power and ranges. Clinical experiments have also been carried out to verify the Monte Carlo simulation results for protons in certain clinical energy ranges.

2 METHODS

2.1 Gafchromic films

Two types of Gafchromic films, EBT3 and EBT-XD, were simulated using Monte Carlo methods. The active layers were selected as the medium for the simulation. The composition of the active layer was as listed in Table 1 (communication with the manufacturer, Ashland, Bridgewater, NJ, USA).

2.2 Monte Carlo methods

Two independent Monte Carlo methods were used in order to cross-check the simulated results: MCNP (MCNP eXtended version 2.5.0)²⁰ and the TRansport of Ions in Matter (TRIM) subroutine in the Stopping and Range of Ions in Matter package (SRIM).²¹ MCNPX is a general-purpose Monte Carlo radiation transport code that tracks nearly all particles at nearly all energies. For the MCNPX simulation, the geometry was a right cylinder with a radius of 1 cm, 30~80-cm long to calculate integral depth dose (IDD) curves. The 1-cm radius was estimated based on the lateral spreading of the proton energy, 350 MeV. As the particle scattered out will not affect the Bragg peak location, a larger size than a 1-cm radius is not necessary. The length was further divided into 100 layers with 3-mm thickness for each layer. For proton CSDA ranges >30 cm or >50 cm, the first layer thickness was adjusted to extend to a thickness of 30 cm or 50 cm to have enough proton transportation length before getting the Bragg peak location for the simulation. The remaining layers still had 3-mm thickness each. The F6 tally (energy deposition averaged over a cell) was used, and 10^7 histories were simulated for each proton energy (50, 55, 60, 65, 70, 75, 80, 85, 90, 95, 100, 125, 150, 175, 200, 225, 250, 275, 300, 350, 400 MeV). A monoenergetic proton pencil beam with no spread out and divergence was incident along with the cylinder length direction in the MCNPX simulation.

SRIM is based on a Monte Carlo simulation method, namely, the binary collision approximation. It is a collection of software packages that calculates many features of the transport of ions in matter. In the SRIM software package, the TRIM subroutine was used for the simulation. One single layer material with 70-cm diameter by default and 70-cm

depth cylinder was used. A total of 1000 particles were simulated, and the software provided the average range with straggle range (the square root of the variance). The other default choices were kept for the calculation: backscattered ions = 0, transmitted ions = 0, and vacancies/ion = 757.9.

In both Monte Carlo code simulations, even though the geometry setups were different, as the purpose was to derive the CSDA range, which was along the center of the geometry, the different geometry will not affect the final CSDA range results.

2.3 Experiments

Experiments with films were also carried out for clinical proton energies to verify the Monte Carlo simulation results. EBT3 and EBT-XD films from the same batches were used for the proton PDD measurements. Two types of measurements were carried out: the surrounding medium was water-equivalent plastic, and the surrounding medium was film-stack. For the water-equivalent medium measurement, the film was placed parallel to the proton beams with a tilt of 5° and 10 × 10 cm² field size, and sandwiched between the Plastic Water (CIRS, Norfolk, VA, USA) slabs (see Figure 1a). The proton energies of 100, 125, 150, 175, 200, and 225 MeV were selected for this determination.

However, to derive the true PDD in film, the exposed EBT3 films were added and used to sandwich two new EBT3 films in the middle to create a phantom containing only film medium. Then the phantom was placed parallel to the proton beams (see Figure 1b). Three proton energies (100, 150, and 200 MeV) frequently used in the clinic were selected for this measurement. The EBT3 film was calibrated by a step-wedge in six-dose level ranging from 65 cGy (relative biological effectiveness) to 250 cGy (relative biological effectiveness,) at depths of 18, 20, and 24 cm in the Plastic Water. Detailed information on the film calibration was documented in our earlier study.²²

2.4 Deriving the mass stopping power

Based on the equation proposed by Newhauser and Zhang,¹⁶ for a given proton energy, the mass stopping power for the film can be derived using the CSDA ranges in water and film, and the mass stopping power of water, as shown in Figure 2 and Equation (1), where S_m is the mass stopping power of the film, t_w is the CSDA range in water, S_w is the mass stopping power of water, ρ_w is the density of water, t_m is the CSDA range in film, and ρ_m is the density of the film. Equation (1) is under the thin targets assumption, where the proton loses a negligible fraction of its energy in the absorber material.¹⁶ For the CSDA range, the distal 50% PDD range can be considered as the CSDA range.¹⁶

$$S_m = \frac{t_w \times S_w \times \rho_w}{t_m \times \rho_m} \quad (1)$$

Because the stopping power was derived using Equation (1), by taking the partial derivative it would give:

$$\frac{\partial S_m}{S_m} = -\frac{\partial t_m}{t_m}, \quad (2)$$

which shows that the relative mass stopping power uncertainties will be equal to the relative CSDA range uncertainties.

3 RESULTS

3.1 Experiment and the MCNPX Monte Carlo simulation results versus ICRU 49 data for water medium

Figure 3a shows the CSDA range comparison among ICRU 49, MCNPX Monte Carlo simulation results, EBT3, and EBT-XD film measurement results in water for the proton energies of 100, 125, 150, 175, 200, and 225 MeV. The Monte Carlo simulation results for the CSDA ranges were derived by using the depth corresponding to the distal 50% of the PDD data, which were linearly interpolated by using distal 80% and 20% of the PDD data. EBT3 and EBT-XD film measurements results were also derived by using the distal 50% of PDD corresponding depth. Comparing the ICRU 49 data for all energies, the average MCNPX Monte Carlo simulation results percentage ratio was 99.7% or 1.4 mm in range; the average percentage ratios for EBT3 and EBT-XD measurement results were 100.8% and 100.7%, respectively; or 1.3 mm difference in range for both EBT3 and EBT-XD films.

3.2 Experiment results for film medium versus the MCNPX and TRIM Monte Carlo simulation for EBT 3 films

Figure 3b shows the measurement results for EBT3 films in EBT3 film medium versus the MCNPX and TRIM Monte Carlo simulation results for the EBT3 film medium. The 50% distal IDD corresponding ranges were used for the CSDA range. The average percentage ratio for MCNPX versus measurement was 98.2% or 3.0 mm in range for the three energies. The average percentage ratio for TRIM versus measurement was 98.9% or 2.4 mm in range for the three energies.

3.3 MCNPX versus TRIM simulation results for CSDA range comparison

Figure 4a shows the calculated CSDA ranges using the MCNPX and TRIM Monte Carlo codes for monoenergetic proton energy from 50 MeV to 400 MeV. The average percentage difference for MCNPX from TRIM was 2.7% for EBT3 film and 4.4% for EBT-XD film.

3.4 MCNPX versus TRIM simulation results for mass stopping power and mass CSDA range

Figure 4b shows the mass stopping power results derived using Equation (1), the ICRU 49 values for liquid water, and the MCNPX calculated CSDA results; CSDA ranges are expressed as g/cm² for EBT 3 and EBT-XD films. The stopping power error bars for MCNPX were calculated based on the CSDA error bars.

3.5 Application examples using the simulated mass stopping power

Stopping power values are the basic physics parameters that can be applied in many fields. One phenomenon observed using film to measure the PDD of protons is the under-response of radiochromic film in the presence of proton spread-out Bragg peaks.^{2,3,11,13,15,23} Figure 5 shows the results for 100, 150, and 200 MeV PDD measurement corrections. Compared with ion chamber measurements, the original film PDD was lower in the Bragg peak region. After applying the EBT3 film to water mass stopping power ratio for the Bragg peak range, the film-measured PDD matched the ion chamber measurement.

Figure 6 shows Monte Carlo simulated 100-MeV proton fluence, energy, and mass stopping power changing with depth in water and EBT3 film. Figure 6a shows that the proton fluence will reduce in a shorter range in EBT3 film than in water. Figure 6b shows that the proton energy will be lost faster in EBT film than in water. Combining the effects of Figures 6a and 6b, Figure 6c shows that the stopping power values are lower in EBT3 than in water, especially in the Bragg peak region. Therefore, it will cause the measured PDD to be lower in EBT3 film than in water.

Tables 2 and 3 show the measured PDD (d_{\max} , d_{90} , d_{50} , d_{20} , d_{10}) values for EBT3 and EBT-XD films sandwiched by the Plastic Water phantom, respectively. The results show that using d_{50} instead of other ranges (such as d_{\max} , d_{90} , d_{20} , or d_{10}) as the CSDA range will cause the range estimate to be within an envelope of about $\pm 3\%$. For lower proton energies (< 100 MeV), the cell thickness plays an important role for the uncertainty; for higher proton energies (>100 MeV), the percent-age dose selection for the range plays an important role.

4 DISCUSSIONS

The mass stopping power has been used for deriving correction factors for proton Bragg spread peak curves measured using the EBT3 and EBT-XD films,^{3,11–13,15,23} correcting the measured dose in water for protons. The data presented here will also provide conversion of the dosimetry measurements in film to another medium if the mass stopping power is available for that medium. Potential applications can also include designing a quality assurance device using film for proton measurements or verifying theory calculations.

In the present study, we used ICRU 49 liquid water stopping power and CSDA data to derive the EBT3 and EBT-XD film data.¹⁷ More recently, ICRU 90 published updated liquid water stopping power and CSDA data¹⁸; however, the stopping power data are within 1% compared with ICRU 49, and the proton energy provided is less than ICRU 49. Therefore, all the liquid water data were from ICRU 49.

For MCNPX Monte Carlo simulation, the dose per cell was recorded and the IDD was plotted. The range of CSDA was estimated by 50% dose corresponding range using linear interpolation of the 80% and 20% PDD data. There are uncertainties in the cell thickness fluctuation recording the dose and IDD for 50% dose estimation by using linear fitting equation. The recording cell thickness was 3 mm, and the maximum uncertainty will be 3 mm (either the particle stopped on the proximal or distal side of the cell). The fact that the 50% distal IDD corresponding range was derived using linear interpolation for MCNPX

simulated CSDA ranges might add uncertainty. Based on Tables 2 and 3, and Equation (2), the range uncertainties are <3 mm maximally for lower energies (<100 MeV) or $<3\%$ maximally for higher energies (>100 MeV).

Instead of calculating the stopping power directly by analytical equations, our approach is to derive the mass stopping power using Equation (1). The Monte Carlo method is an indirect method in conjunction with the use of the published data for water in ICRU 49. Hence, it is only required to simulate the CSDA results for film, which it is straightforward and relatively simpler than using analytical methods. Plus, the range uncertainties for the simulation are transferred to the stopping power uncertainties, as we analyzed. Therefore, the stopping power data should have already had the built-in uncertainties.

The stopping powers for Gafchromic EBT3 and EBT-XD films for monoenergetic proton energies ranging from 50 to 400 MeV were derived based on the Monte Carlo simulation of the CSDA range in the films, the use of ICRU 49 data of the CSDA range, and the stopping power in water. Comparison of MCNPX, TRIM, and measurement results in water and film agreed with each other within a certain tolerance. The derived mass stopping power can be implemented in many areas of basic and applied radiotherapy physics, such as correcting the quenching effects of EBT3 and EBT-XD film dosimetry, as shown in the present work.

ACKNOWLEDGMENTS

This work was supported in part by the National Institutes of Health and National Cancer Institute [P30 CA008748] and Ashland Specialty Ingredients [#SKI-11069].

Funding information

NIH/NCI Cancer Center, Grant/Award Number: P30 CA008748

REFERENCES

1. Sutherland JGH, Rogers DWO. Monte Carlo calculated absorbed-dose energy dependence of EBT and EBT2 film. *Med Phys* 2010;37:1110-1118. doi:10.1118/1.3301574. [PubMed: 20384246]
2. Zhao L, Das IJ. Gafchromic EBT film dosimetry in proton beams. *Phys Med Biol* 2010;55:N291-N301. doi:10.1088/0031-9155/55/10/N04. [PubMed: 20427858]
3. Kirby D, Green S, Palmans H, Hugtenburg R, Wojnecki C, Parker D. LET dependence of GafChromic films and an ion chamber in low-energy proton dosimetry. *Phys Med Biol* 2010;55:417-433. doi:10.1088/0031-9155/55/2/006. [PubMed: 20019399]
4. Dreindl R, Georg D, Stock M. Radiochromic film dosimetry: considerations on precision and accuracy for EBT2 and EBT3 type films. *Med Phys* 2014;41:153-163. doi:10.1016/j.zemedi.2013.08.002. Epub 2013 Sep 20.
5. Grams MP, Gustafson JM, Long KM, de los Santos LEF. Technical Note: initial characterization of the new EBT-XD Gafchromic film. *Med Phys* 2015;42:5782-5786. [PubMed: 26429252]
6. Palmer AL, Dimitriadis A, Nisbet A, Clark CH. Evaluation of Gafchromic EBT-EBT-XD film, with comparison to EBT3 film, and application in high dose radiotherapy verification. *Phys Med Biol* 2015;60:8741-8752. doi:10.1088/0031-9155/60/22/8741. [PubMed: 26512917]
7. Lewis DF, Chan MF. Technical Note: on GAFChromic EBT-XD film and the lateral response artifact. *Med Phys* 2016;43:643-649. [PubMed: 26843228]
8. Schoenfeld AA, Wieker S, Harder D, Poppe B. Changes of the optical characteristics of radiochromic films in the transition from EBT3 to EBT-XD films. *Phys Med Biol* 2016;61:5426-5442. [PubMed: 27367839]

9. Schoenfeld AA, Wieker S, Harder D, Poppe B. The origin of the flatbed scanner artifacts in radiochromic film dosimetry—key experiments and theoretical descriptions. *Phys Med Biol* 2016;61:7704–7724. [PubMed: 27740945]
10. Miura H, Ozawa S, Hosono F, et al. Gafchromic EBT-XD film: dosimetry characterization in high-dose, volumetric-modulated arc therapy. *J Applied Clin Med Phys* 2016;17:312–322.
11. Perles LA, Mirkovic D, Anand A, Titt U, Mohan R. LET dependence of the response of EBT2 films in proton dosimetry modeled as a bimolecular chemical reaction. *Phys Med Biol* 2013;58:8477–8491. 10.1088/0031-9155/58/23/8477. [PubMed: 24240474]
12. Goma C, Andreo P, Sempau J. Spencer-Attix water/medium stopping-power ratios for the dosimetry of proton pencil beams. *Phys Med Biol* 2013;58:2509–2522. 10.1088/0031-9155/58/8/2509. [PubMed: 23514896]
13. Fiorini F, Kirby D, Thompson J, et al. Under-response correction for EBT3 films in the presence of proton spread out Bragg peaks. *Phys Med* 2014;30:454–461. 10.1016/j.ejmp.2013.12.006. Epub 2014 Jan 22. [PubMed: 24461335]
14. Jung H, Kum O, Han Y, Park B, Cheong KH. Photon Beam Dosimetry with EBT3 Film in Heterogeneous Regions: application to the Evaluation of Dose-calculation Algorithms. *J Korean Physical Society* 2014;65:1829–1838.
15. Battaglia MC, Schardt D, Espino JM, et al. Dosimetric response of radiochromic films to protons of low energies in the Bragg peak region. *Phys Accel Beams* 2016;19 <https://doi.org/10.1103/PhysRevAccelBeams.19.064701>. 064701-(1-7).
16. Newhauser WD, Zhang R. The physics of proton therapy. *Phys Med Biol* 2015;60:R155–R209. 10.1088/0031-9155/60/8/R155. [PubMed: 25803097]
17. ICRU, Stopping Powers and Ranges for Protons and Alpha Particles Report No. 49, International Commission on Radiation Units and Measurements, Bethesda, MD (1993).
18. ICRU, Key Data for Ionizing-Radiation Dosimetry: Measurement Standards and Applications Report No. 90, International Commission on Radiation Units and Measurements, Bethesda, MD (2016).
19. Zhang R, Newhauser. Calculation of water equivalent thickness of materials of arbitrary density, elemental composition and thickness in proton beam irradiation. *Phys Med Biol* 2009;54:1383–1395. 10.1088/0031-9155/54/6/001. [PubMed: 19218739]
20. MCNPX™ user's manual, version 2.5.0 LA-CP-05-0369 (2005).
21. Ziegler JF, Ziegler MD, Biersack JP. SRIM—The stopping and range of ions in matter. *Nuclear Instruments and Methods in Physics Research* 2010;B 268:1818–1823.
22. Chan MF, Chen CC, Shi C, et al. Patient-specific QA of spot-scanning proton beams using radiochromic film. *Int J Med Phys Clinic Eng Radiat Oncol* 2017;6:111–123.
23. Castriconi R, Ciocca M, Mirandola A, et al. Dose-response of EBT3 radiochromic films to proton and carbon ion clinical beams. *Phys Med Biol* 2017;62:377–393. 10.1088/1361-6560/aa5078.21. Epub 2016 Dec 20. [PubMed: 27997377]

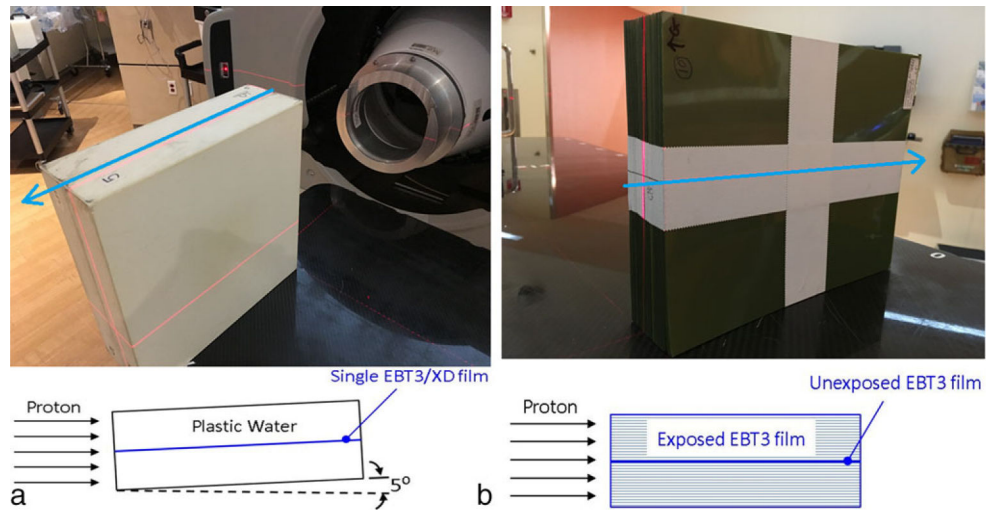


FIGURE 1. Experiment setup illustration in the (a) film sandwiched by two Plastic Water blocks and tilted by 5°; (b) film sandwiched by exposed film blocks and placed parallel to the beam direction. Note that arrows in pictures show the proton beam direction

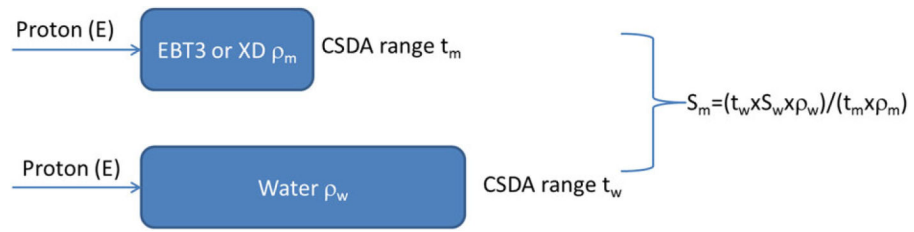


FIGURE 2. Illustration of the stopping power equation. CDSA, continuous slowing down approximation

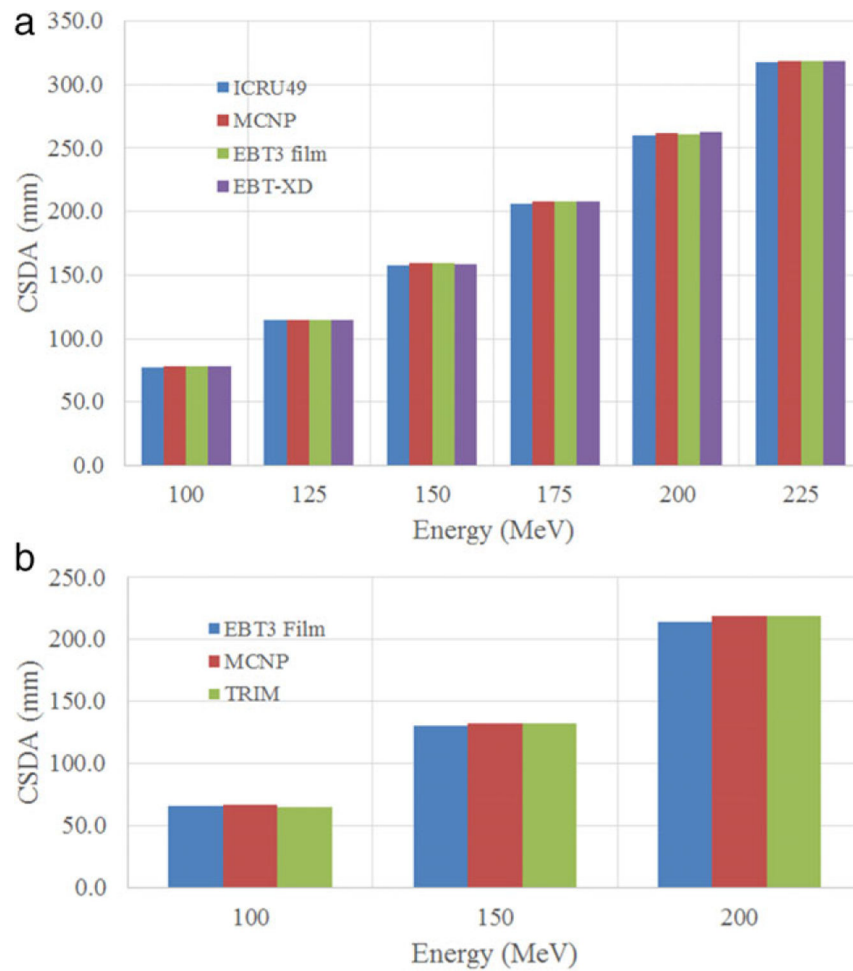


FIGURE 3.

(a) Comparison of continuous slowing down approximation (CSDA) range in water among International Commission on Radiation Units and Measurement (ICRU) 49, MCNPX simulation results, EBT3, and EBT-XD film measurement; (b) comparison of CSDA range in film among MCNPX, TRansport of Ions in Matter (TRIM) simulation results, and EBT3 film measurement

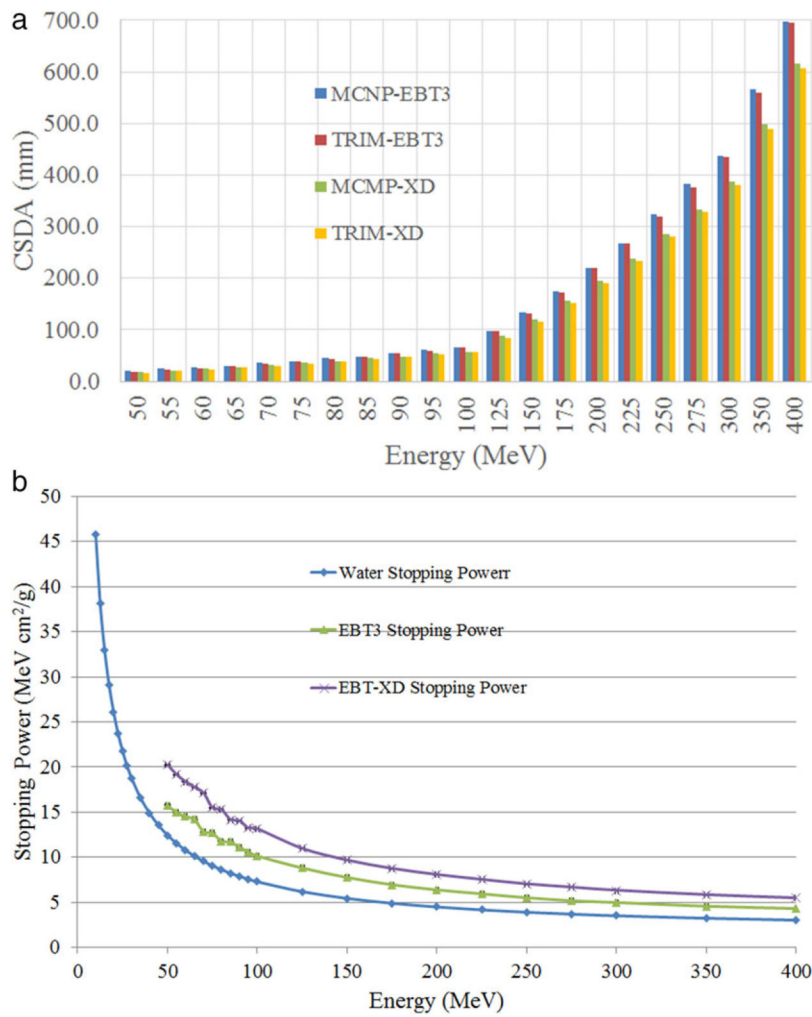


FIGURE 4. (a) Continuous slowing down approximation (CSDA) range comparison for MCNPX versus TRansport of Ions in Matter (TRIM) for EBT3 and XD film; (b) MCNPX results for stopping power of EBT3 and EBT-XD films versus International Commission on Radiation Units and Measurement (ICRU) 49 water stopping power

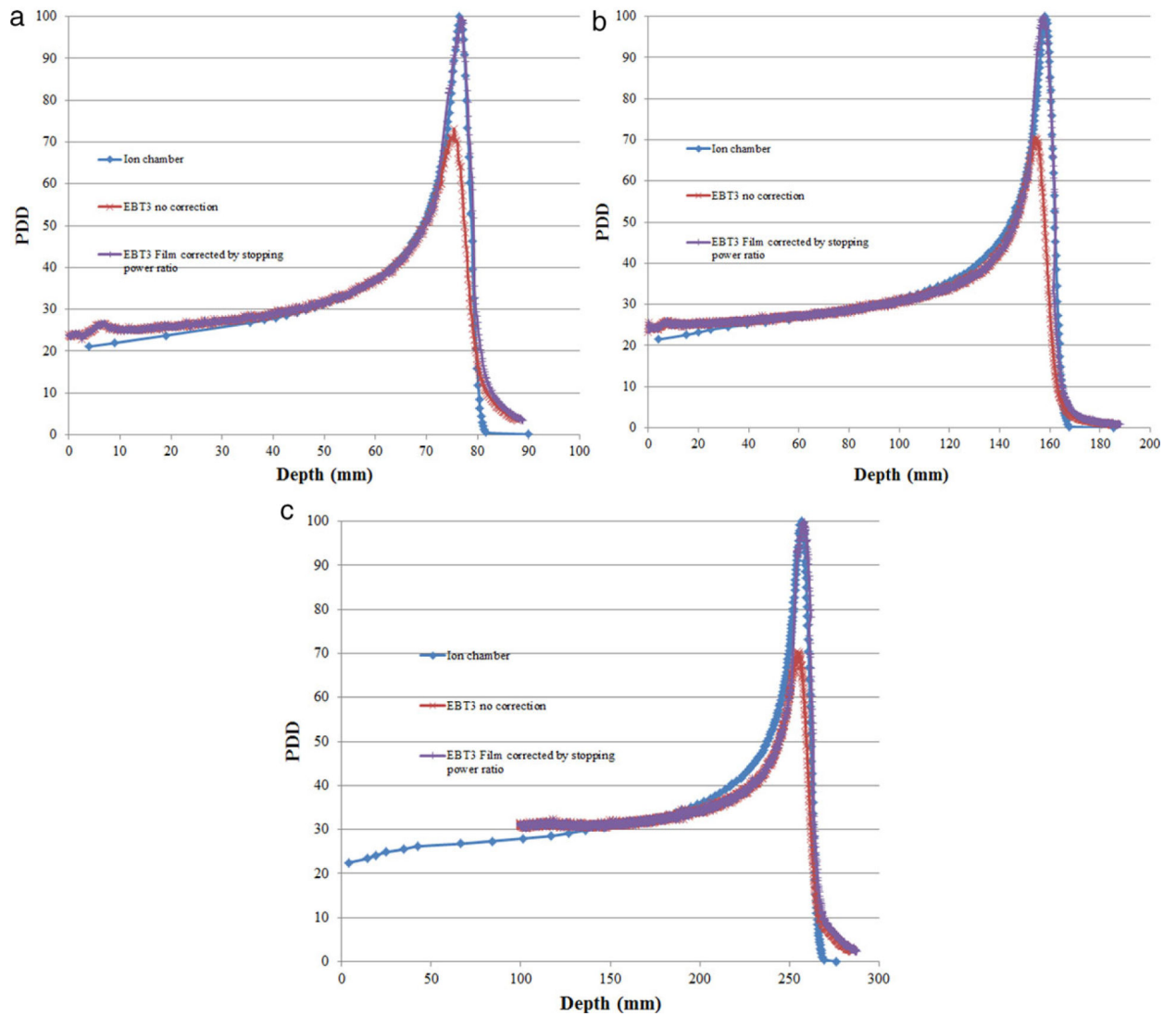


FIGURE 5. Examples of the mass stopping power ratio applications in EBT film percentage depth doses (PDD) correction: (a) 100-MeV proton measurement; (b) 150-MeV proton measurement; and (c) 200-MeV proton measurement. No measurement less than the first 10-cm depth is presented for film, as the range is larger than the film's dimension

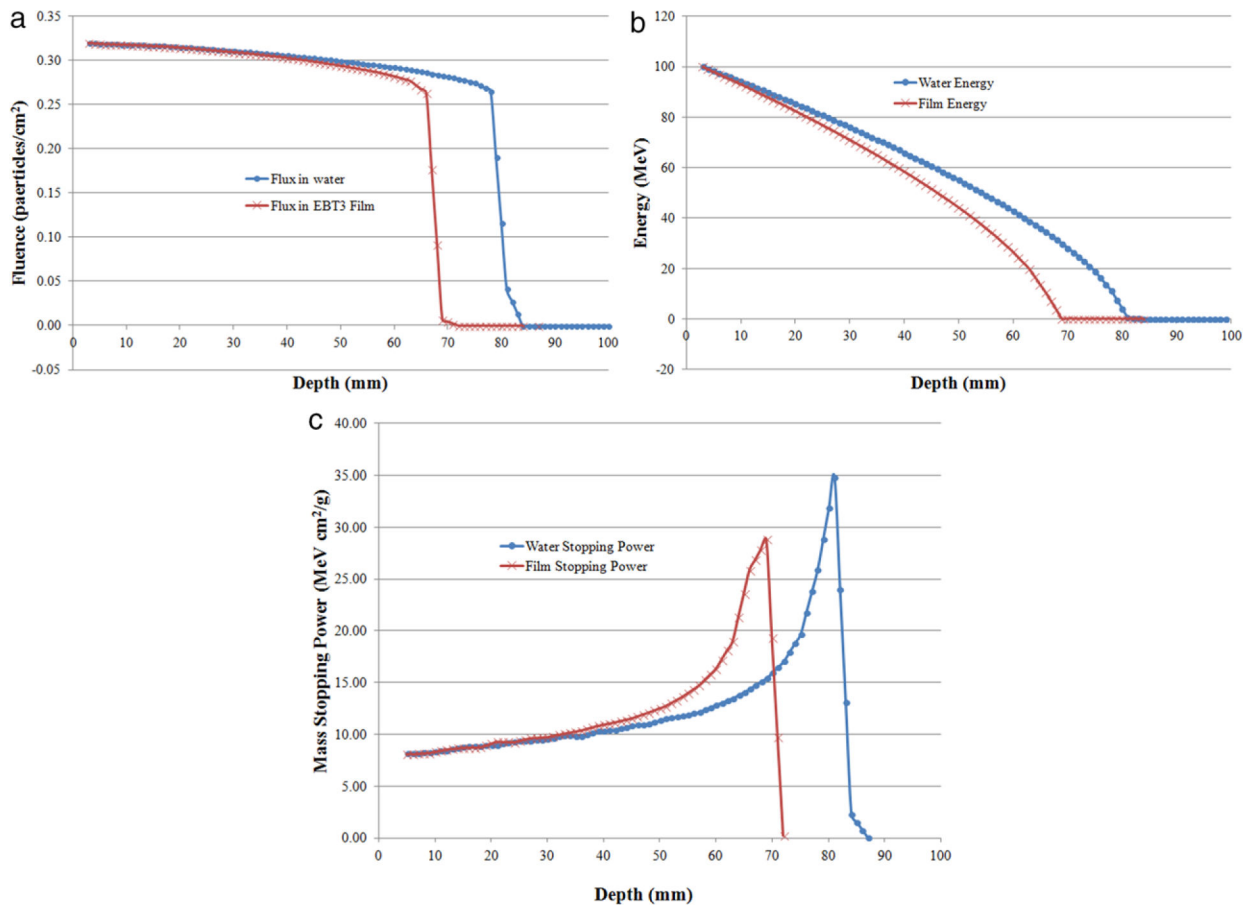


FIGURE 6. (a) Change of proton fluence in EBT3 and water with depth. (b) Change of proton energy in EBT3 and water with depth. (c) Change of EBT3 and water stopping power with depth

Table 1

EBT3 and EBT-XD film composition information for the Monte Carlo simulation

Active layer	Density (g/cm ³)	Composition (atomic percentage)								
		H	Li	C	N	O	Na	Al	S	Cl
EBT3	1.20	56.9	0.6	27.6	Null	13.3	Null	1.6	Null	Null
EBT-XD	1.35	57.0	0.6	28.6	0.4	11.7	0.1	1.4	0.1	0.1

Author Manuscript

Author Manuscript

Author Manuscript

Author Manuscript

Table 2
Measured ranges for EBT3 film percentage depth doses in Plastic Water, and the percent ratios of D_{50}

Energy (MeV)	d_{max}	d_{max}/d_{50}	d_{90}	d_{90}/d_{50}	d_{50}	d_{20}	d_{20}/d_{50}	d_{10}	d_{10}/d_{50}
100	75.7	96.6%	76.7	97.8%	78.4	80.5	102.7%	83.7	106.8%
125	110.2	96.1%	112.3	97.9%	114.7	116.8	101.8%	118.9	103.7%
150	154.3	96.8%	156.5	98.2%	159.4	162.0	101.6%	164.3	103.1%
175	203.2	97.6%	204.7	98.3%	208.3	211.2	101.4%	213.5	102.5%
200	254.3	97.3%	257.6	98.6%	261.3	265.1	101.5%	271.5	103.9%
225	310.1	97.4%	314.4	98.7%	318.4	322.0	101.1%	324.8	102.0%

The unit of the range is in mm

TABLE 3
 Measured ranges for XD film percentage depth doses in Plastic Water, and the percent ratios of D_{50}

Energy (MeV)	d_{max}	d_{max}/d_{50}	d_{90}	d_{90}/d_{50}	d_{50}	d_{20}	d_{20}/d_{50}	d_{10}	d_{10}/d_{50}
100	75.4	96.4%	76.2	97.4%	78.2	80.0	102.3%	81.3	104.0%
125	110.5	96.5%	112.4	98.2%	114.5	116.0	101.3%	117.0	102.2%
150	153.5	96.8%	156.0	98.4%	158.6	160.3	101.1%	161.0	101.5%
175	202.2	97.3%	204.7	98.5%	207.8	209.8	101.0%	210.7	101.4%
200	255.3	97.3%	258.9	98.7%	262.3	265.0	101.0%	266.5	101.6%
225	312.2	97.9%	315.3	98.9%	318.8	321.3	100.8%	322.5	101.2%

The unit of the range is in mm